3D Freeform Millimeter-Wave and THz Structures Based on Multi-Photon Lithography

Pascal Maier[1,2], Alexander Kotz[1], Joachim Hebeler[3], Qiaoshuang Zhang[4], Christian Benz[1,2], Alexander Quint[3], Marius Kretschmann[3], Tobias Harter[1], Sebastian Randel[1], Uli Lemmer[4], Wolfgang Freude[1], Thomas Zwick[3], Christian Koos[1,2,5,6]

[1] *Institute of Photonics and Quantum Electronics (IPQ), Karlsruhe Institute of Technology (KIT), Engesserstr. 5, 76131 Karlsruhe, Germany*
[2] *Institute of Microstructure Technology (IMT), KIT, Hermann-von-Helmholtz-Platz 1, 76344 Eggenstein-Leopoldshafen, Germany*
[3] *Institute of Radio Frequency Engineering and Electronics (IHE), KIT, Engesserstr. 5, 76131 Karlsruhe, Germany*
[4] *Light Technology Institute (LTI), KIT, Engesserstr. 13, 76131 Karlsruhe, Germany*
[5] *Vanguard Automation GmbH, Gablonzer Str. 10, 76185 Karlsruhe, Germany*
[6] *Keystone Photonics GmbH, Gablonzer Str. 10, 76185 Karlsruhe, Germany*
pascal.maier@kit.edu, christian.koos@kit.edu

Abstract: We exploit high-resolution multi-photon lithography for fabricating 3D-freeform millimeter-wave and THz structures that overcome the limitations of conventional planar architectures. We demonstrate THz probes, suspended antennas, and ultra-broadband chip-chip interconnects offering bandwidths in excess of 0.3 THz. © 2024 The Author(s)

1. Introduction

High-performance millimeter-wave (mmW) and terahertz (THz) structures are key to future wireless and optical transceivers, where carrier frequencies of hundreds of GHz and symbol rates of 200 GBd or more are anticipated [1,2]. On a technical level, functional mmW and THz structures crucially rely on precisely defined three-dimensional (3D) freeform geometries that combine highly conducting metal elements with low-loss dielectrics. Geometrical precision and essentially arbitrary 3D shapes can be achieved by direct-write multi-photon laser lithography, offering highest resolution on the sub-micrometer scale along with precise alignment of the fabricated structures with respect to existing circuitry on the underlying substrates. These advantages have been extensively exploited in the realm of photonic integration, where 3D-printed waveguides, so-called photonic wire bonds (PWB) [3,4], or facet-attached microlenses (FaML) [5,6] offer interesting perspectives for highly scalable fully automated assembly of hybrid multi-chip systems. However, transferring these concepts to mmW and THz assemblies has so far been hindered by the lack of microfabrication techniques that produce precisely defined highly conductive metal elements. Previously demonstrated approaches towards 3D nano-printing of metals relied on two-photon-induced reduction of metal salts [7] or on simultaneous two-photon polymerization and photoreduction to yield gold-containing 3D nanocomposites [8]. However, the achievable electrical conductivity of the resulting structures is limited by the metal loading of the respective photoresist, which is inherently limited, e.g., by the solubility of the metal ions in the photoresist. On the other hand, a combination of physical vapor deposition (PVD) techniques and subsequent electroplating allows to globally cover 3D-printed polymer templates with highly conductive metal coatings [9]. However, this concept cannot offer highly precise localized deposition and has therefore mainly been used for bulky stand-alone hollow-core waveguides or horn antennas, that require additional mechanical assembly steps to yield functional mmW or THz elements.

In this paper, we introduce and experimentally demonstrate a novel approach that allows to leverage multi-photon lithography for fabricating high-performance mmW and THz structures with hitherto unachieved precision and functionality. Our concept exploits precisely localized conductive coating of *in-situ* printed polymer templates, obtained through highly directive metal deposition techniques in combination with 3D-printed shadowing structures. The resulting metal-coated freeform structures (MCFS) offer high surface quality, low dielectric losses in the polymer base structure, and high conductivities close to those of bulk metal in the coating, while alleviating the need for additional mechanical assembly steps. We experimentally prove the viability of our concept in a series of experiments, comprising THz interconnects that bridge the gap between transmission lines on different planar substrates and that offer record-high bandwidths in excess of 0.3 THz as well as advanced THz probes and suspended THz antennas with unprecedented geometrical 3D design freedom. We believe that our concept paves a path towards advanced mmW and THz components and assemblies for communications, sensing, or ultra-broadband signal processing.

2. Concept and Fabrication

The basic concept of 3D-printed metal-coated freeform structures (MCFS) is shown in Fig. 1 along with potential use cases. As an example, we sketch an optoelectronic THz system that relies on a photonic integrated circuit (PIC) with a balanced pair of high-speed photodetectors acting as a THz signal source [10] and that further comprises a THz amplifier based on a monolithic microwave integrated circuit (MMIC) and a THz antenna, which is suspended from the surface of the underlying high-index substrate for efficient emission to the surface-normal direction. The THz chip-chip interconnect between the PIC and MMIC as well as the suspended THz antenna are implemented as MCFS. Each MCFS consists of a 3D-printed polymeric support that is locally coated with metal layers offering high bulk conductivity along with mmW-grade surface quality. The same concept can be used to implement THz probes with unprecedented precision and geometrical design freedom, that lend themselves to testing of mmW and THz integrated circuits, see upper part of Fig. 1(a). Micrographs of functional MCFS are shown in Fig. 1(b), (c) and (d). Figure 1(b) shows a THz chip-chip interconnect (TIC) bridging the gap between coplanar waveguide (CPW) transmission lines on different substrates (Al_2O_3), Fig. 1(c) shows a THz probe that is turned upside down for better visibility, and Fig. 1(d) shows a suspended THz antenna.

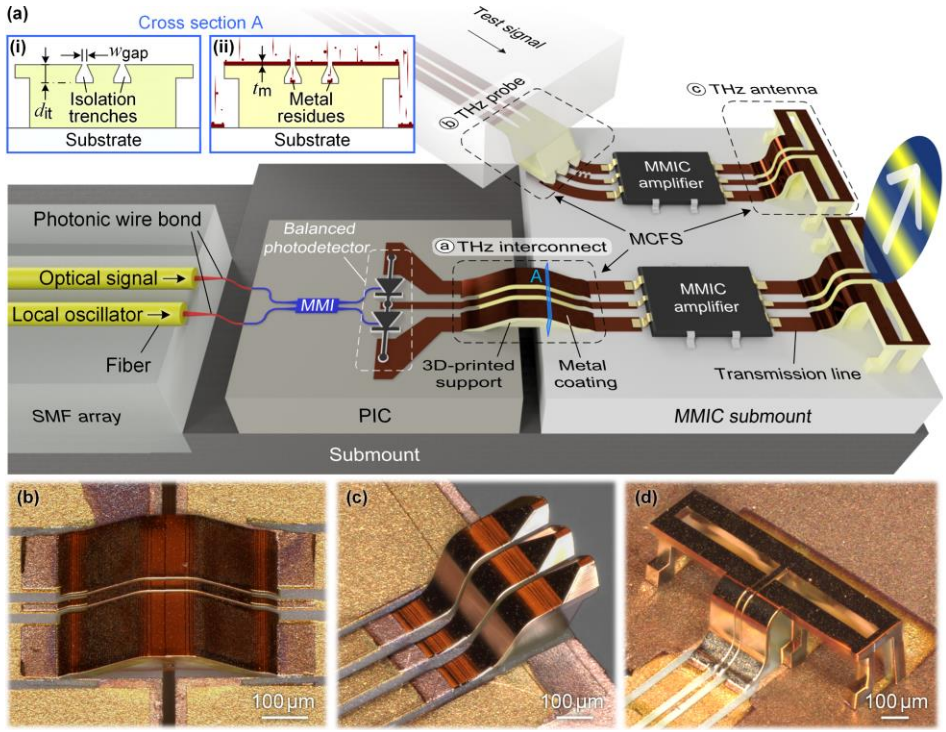

Fig. 1: Concept and implementation of 3D-printed metal-coated freeform structures (MCFS), illustrated for an exemplary optoelectronic THz system. Each MCFS consists of a 3D-printed polymeric support that is coated with precisely localized metal structures. **(a)** MCFS-based optoelectronic THz system. The system relies on a photonic integrated circuit (PIC) with a balanced pair of high-speed photodetectors acting as a THz signal source and further comprises a THz amplifier based on a monolithic microwave integrated circuit (MMIC) and a suspended THz antenna. The PIC contains a series of functional photonic structures such as multi-mode-interference (MMI) couplers and is fed with an optical signal and an optical local-oscillator tone via an array of single-mode fibers (SMF). The THz chip-chip interconnect (TIC) between the PIC and MMIC as well as the suspended THz antenna are implemented as MCFS. The same concept can be used to implement THz probes with unprecedented precision and geometrical design freedom. The fabrication of the MCFS relies on a multi-step process, which is illustrate by the cross-sectional view A of the TIC, see Insets (i) and (ii). In a first step, polymer support structures are 3D-printed using *in-situ* multi-photon lithography, see Inset (i). The support structures contain isolation trenches with undercut sidewalls, which separate the metal strips that are obtained by directive metal coating from the surface-normal direction and that may form a ground-signal-ground (GSG) transmission line, see Inset (ii). Additional roof-like 3D-printed shadowing structures (not shown) can be used to avoid metal deposition in certain areas. The surface of the freeform structures is designed to support a metal layer (thickness $t_m = (0.5 \ldots 1.5)\,\mu m$), which connects smoothly to the CPW on the substrate, and which maintains a constant line impedance of, e.g., 50 Ω along the transmission line by continuously adapting the width of the gaps in the range $w_{gap} = (3 \ldots 30)\,\mu m$. Unavoidable metal residues at the ground of the isolation trenches do not influence the characteristics of the MCFS-based TIC if the isolation trenches are designed with sufficient depth $d_{it} \geq 20\ \mu m$. Note that the concept can be efficiently combined with 3D-printed optical connections such as photonic wire bonds (PWB). **(b)** Micrograph of a TIC bridging the gap between CPW on different planar substrates. **(c)** Micrograph of a THz probe that is turned upside down for better visibility. **(d)** Micrograph of a suspended THz antenna for efficient radiation to the surface-normal direction.

The fabrication of the MCFS relies on a multi-step process, which we illustrate using the cross-sectional view A of the TIC as illustrated in Fig. 1(a) and in the associated Insets (i) and (ii). In a first step, polymer support structures are 3D-printed with sub-micrometer precision using direct-write multi-photon lithography, see Inset (i). The flexibility offered by *in-situ* laser printing allows to adapt the shape of the support structure to the position of the underlying mmW or THz chips, thereby alleviating the need for costly high-precision alignment steps. The support structures contain isolation trenches with undercut sidewalls, see Inset (ii) of Fig. 1(a), which separate the ground and the signal metal strips that are obtained by directive PVD-based metal coating from the surface-normal direction. The metal coating typically consists of several layers, comprising Cu as the main conductor, an underlying Ti or Al layer for adhesion promotion, and a Ti/Au diffusion and oxidation protection on top. The surface of the freeform structures is designed to support a metal layer which connects smoothly to the CPW on the substrate and which maintains a constant line impedance of, e.g., 50 **Ω** along the entire ground-signal-ground (GSG) transmission line. For protecting the planar THz structures on the underlying substrates during the global metal deposition, the associated areas of the substrates are temporarily covered by a PMMA film (not shown) using inkjet printing. At the transitions between the PMMA-covered planar substrate and the 3D freeform polymeric support, additional 3D-printed shadowing structures (not shown) are used to prevent short circuits. After metal deposition, the sacrificial PMMA and the shadowing structures are removed, thereby discarding the unwanted metal areas and leaving the final MCFS in Fig. 1(b), (c) and (d). To verify the high conductivity and surface quality of the deposited metal layers, we analyzed various fabricated MCFS. The surface roughness was measured using a white-light interferometer, revealing a root-mean-squared surface roughness of $R_{\mathrm{q,MCFS}} = (13 \ldots 14)\,\mathrm{nm}$, slightly larger than the roughness of the underlying 3D-printed support of $R_{\mathrm{q,support}} = (9 \ldots 10)\,\mathrm{nm}$. The conductivity of the metal films was extracted from four-wire measurements of metal strips, which were separately fabricated on planar substrates using the same evaporation processes and metal layer stacks. Assuming a homogeneous metal layer for simplicity, we extract an effective conductivity of $\sigma_{\mathrm{MCFS}} = (3.29 \pm 0.12) \times 10^{7}\,\mathrm{S/m}$. This corresponds to $(57 \pm 2)\%$ of the bulk material value of copper and is consistent with previously reported values using similar deposition techniques [11]. The slight conductivity reduction compared to bulk material is a known effect related to the grain boundaries of the deposited metal layers [11,12], which might be mitigated by further process optimization.

3. Demonstration of ultra-broadband chip-chip interconnects

To prove the viability of our concept, we performed a series of experiments which were geared towards demonstration of the building blocks shown in Fig. 1(b), (c) and (d). Here, we exemplarily show the results for an ultra-broadband MCFS-based TIC as depicted in Fig. 1(b). Figure 2 shows the associated de-embedded transmission characteristics $S_{21,\mathrm{dB}} = 10\log_{10}(|\underline{S}_{21}|^2)$ (green line) of the THz chip-chip interface, revealing a 3 dB-bandwidth beyond the 0.330 THz measurement range of our equipment. The measured characteristics show excellent agreement with simulations (dashed black line) obtained from a numerical time-domain solver (CST Microwave Studio, Dassault Systèmes). Note that the measured *S*-parameters had to be acquired separately in different frequency ranges using dedicated signal sources, waveguides, and probes, thereby leaving a gap between 0.170 THz and 0.200 THz, where no adequate signal sources were available. To the best of our knowledge, these experiments represent the first demonstration of an additively manufactured ultra-broadband chip-chip interconnect, offering a record-high bandwidth in excess of 0.3 THz. Competing approaches comprise aerosol-jet-printed conductive lines deposited on dielectric ramps [13] or epoxy underfills [14], as well as lithographically defined self-aligning metal nodules [15], that require subsequent reflow fusing or electroless plating processes. However, these approaches have only been demonstrated up to 0.22 THz in few cases [13,15] and generally lack the precision and design flexibility offered by the presented MCFS concept. We have also fabricated and tested MCFS-based THz probes and suspended THz antennas, revealing comparable bandwidth performance.

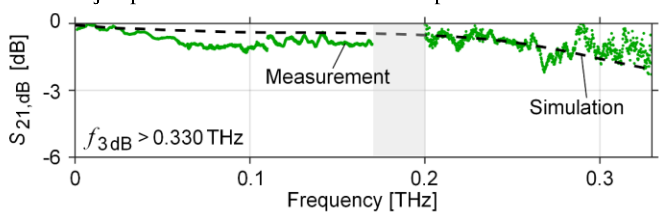

Fig. 2: De-embedded transmission characteristics $S_{21,\mathrm{dB}} = 10\log_{10}(|\underline{S}_{21}|^2)$ (green line) of an MCFS-based THz chip-chip interconnect (TIC, see Fig. 1(b)). The 3 dB-bandwidth is beyond the 0.330 THz measurement range of our equipment, and the measured characteristics show excellent agreement with simulations (dashed black line).

4. Summary

We have introduced and experimentally demonstrated a novel concept for fabricating precisely defined mmW and THz structures, relying on *in-situ* printing of freeform polymer support structures and precisely localized coating through highly directive metal deposition techniques. The resulting metal-coated freeform structures (MCFS) offer high surface quality in combination with conductivities comparable to bulk material values and do not require any manual assembly steps. We experimentally prove the viability of our concept in a series of experiments, comprising THz interconnects that bridge the gap between transmission lines on different planar substrates and that offer record-high bandwidths in excess of 0.3 THz as well as advanced THz probes and suspended THz antennas with unprecedented geometrical design freedom in three dimensions. We believe that our concept paves a path towards advanced mmW and THz components and assemblies for communications, sensing, or ultra-broadband signal processing.

This work was supported by the Deutsche Forschungsgemeinschaft (DFG, German Research Foundation) via the Excellence Cluster 3D Matter Made to Order (EXC-2082/1 – 390761711), via the DFG Collaborative Research Center HyPERION (SFB 1527), and via the projects PACE (# 403188360) and GOSPEL (# 403187440) within the Priority Programme "Electronic-Photonic Integrated Systems for Ultrafast Signal Processing" (SPP 2111), by the ERC Consolidator Grant TeraSHAPE (# 773248), by the EU Horizon 2020 project TeraSlice (# 863322), by the European Innovation Council (EIC) transition project HDLN (# 101113260), by the BMBF project Open6GHub (# 16KISK010), by the Alfried Krupp von Bohlen und Halbach Foundation, and by the Karlsruhe School of Optics & Photonics (KSOP).

References

[1] P. Sen, *et al.* "Multi-kilometre and multi-gigabit-per-second sub-terahertz communications for wireless backhaul applications," Nat Electron **6**, 164–175 (2023).
[2] Yole Intelligence, "Market and technology trends – Optical transceivers for datacom and telecom 2023," (2023).
[3] M. Blaicher, *et al.* "Hybrid multi-chip assembly of optical communication engines by *in situ* 3D nano-lithography," Light Sci Appl **9**, 71 (2020).
[4] A. Nesic, *et al.* "Ultra-broadband polarisation beam splitters and rotators based on 3D-printed waveguides," Light: Advanced Manufacturing **4**, 22 (2023).
[5] Y. Xu, *et al.* "3D-printed facet-attached microlenses for advanced photonic system assembly," Light: Advanced Manufacturing **4**, 3 (2023).
[6] P. Maier, *et al.* "3D-printed facet-attached optical elements for connecting VCSEL and photodiodes to fiber arrays and multi-core fibers," Opt Express **30**, 46602–46625 (2022).
[7] L. Yang, *et al.* "Laser printed microelectronics," Nat Commun **14**, 1103 (2023).
[8] Q. Hu, *et al.* "Additive manufacture of complex 3D Au-containing nanocomposites by simultaneous two-photon polymerisation and photoreduction," Sci Rep **7**, 17150 (2017).
[9] R. Xu, *et al.* "A review of broadband low-cost and high-gain low-terahertz antennas for wireless communications applications," IEEE Access **8**, 57615–57629 (2020).
[10] T. Harter, T., *et al.* "Silicon–plasmonic integrated circuits for terahertz signal generation and coherent detection," Nature Photon **12**, 625–633 (2018).
[11] A. Emre Yarimbiyik, *et al.* "Experimental and simulation studies of resistivity in nanoscale copper films," Microelectronics Reliability **49**, 127–134 (2009).
[12] K. S. Sree Harsha, "Nucleation and Growth of Films," Principles of Vapor Deposition of Thin Films 685–829 (2006).
[13] M. Ihle, *et al.* "Functional printing of MMIC-interconnects on LTCC packages for sub-THz applications," in *European Microelectronics and Packaging Conference & Exhibition (EMPC)* (IEEE, 2019), pp. 1–4.
[14] M. T. Craton, *et al.* "Additive manufacturing of a wideband capable W-band packaging strategy," IEEE Microwave and Wireless Components Letters **31**, 697–700 (2021).
[15] P. Fay, *et al.* "Ultra-wide bandwidth inter-chip interconnects for heterogeneous millimeter-wave and THz circuits," J Infrared Millim Terahertz Waves **37**, 874–880 (2016).